International Journal of Signal Processing, Image Processing and Pattern Recognition
Vol.9, No.2 (2016), pp.421-432
http://dx.doi.org/10.14257/ijsip.2016.9.2.36

Performance Analysis of Switched Diversity Combining System

Lingwei Xu[1], Jingjing Wang[1], Hao Zhang[2,3] and T. Aaron Gulliver[3]

[1]*Department of Information Science and Technology, Qingdao University of Science and Technology, Qingdao 266061, China*
[2]*College of Information Science and Engineering, Ocean University of China, Qingdao 266100, China*
[3]*Department of Electrical and Computer Engineering, University of Victoria, Victoria V8W 2Y2, Canada*

Abstract

The average symbol error probability (ASEP) and outage probability (OP) performance of the switched diversity combining (SDC) system over N-Nakagami fading channels is investigated in this paper. The probability density function (PDF) of the signal-to-noise ratio (SNR) is used to derive exact and approximate ASEP expressions for phase shift keying (PSK) and pulse amplitude modulation (PAM). Exact closed-form expressions for OP of the SDC system are also presented. The ASEP and OP performance under different conditions is evaluated through numerical simulation to verify the analysis. Results are presented which show that the performance of the SDC system is improved when the number of diversity branches and the fading coefficient is increased, but is degraded as the number of cascaded components is increased.

Keywords: *M2M communication; switched diversity combining; N-Nakagami fading channels; probability density function; average symbol error probability; outage probability*

1. Introduction

In recent years, mobile application development is swiftly expanding due to the popularity of streaming video, gaming, and other social media services [1]. Mobile-to-mobile (M2M) communication has attracted wide research interest from both academic and industrial fields. M2M communication is widely employed in many popular wireless communication systems, such as mobile ad-hoc networks, intelligent highway applications and mobile ad-hoc applications [2]. However, the classical Rayleigh, Rician, or Nakagami fading channels have been found not to be applicable in M2M communication. When both the transmitter and receiver are moving, the channel can be characterized by a double-Rayleigh fading model in [3]. Afterwards, *N*-Nakagami channel is adopted to provide a realistic description of the M2M channel in [4]. 2-Nakagami is a special case of *N*-Nakagami with *N*=2. The exact symbol error rate (SER) and asymptotic SER expressions for the decode-and-forward (DF) relaying M2M system over 2-Nakagami fading channels are derived in [5].

As a promising solution for the high data-rate coverage required in M2M communication systems, multiple-input multiple-output (MIMO) technology has attracted wide research interest [6]. It has been shown that MIMO technology can provide the high capacity and spatial diversity required for next generation wireless systems [7-9]. To improve the spectral efficiency and reliability of wireless communications over fading channels, spatial diversity schemes are widely employed in MIMO systems. These include maximal ratio combining (MRC), equal gain combining (EGC), and selection combining (SC). Unfortunately, MRC and EGC require channel state information, such as the fading amplitude and phase for the received signals to be combined, which can be

ISSN: 2005-4254 IJSIP

difficult to obtain. Conversely, SC only employs one of the diversity branches, and so is a low complexity solution. However, SC is impractical for systems that have uninterrupted transmission, such as frequency division multiple access (FDMA) systems, since simultaneous and continuous monitoring of the channels is required. Hence, switched diversity combining (SDC) is often implemented to solve this problem [10]. From a signal processing perspective, SDC is simpler to implement than MRC, EGC, or SC, because an SDC combiner only needs to monitor and process one of the L diversity branches. The most widely employed SDC techniques are switch-and-stay combining (SSC) and switch-and-examine combining (SEC). Using the moment generating function (MGF) approach, the average bit error rate (BER) performance of a dual SSC diversity receiver over correlated generalized-K (KG) fading channels was analyzed in [11]. Exact closed-form analytical expressions for the average BER of a multi-branch SEC diversity system over independent and identically Nakagami-m distributed fading channels were derived in [12]. Using the MGF method, the average BER performance of a dual-branch SSC diversity system over κ-μ fading channels was investigated in [13].

However, to the best knowledge of the author, the performance of an SDC system over N-Nakagami fading channels has not yet been examined. In [11-13], most results on the performance of diversity techniques employ the MGF method, while the probability density function (PDF) of the SNR is largely ignored. Motivated by all of the above, in this paper, the PDF of the SNR is used to derive exact expressions for the average symbol error probability (ASEP) of an SDC system over N-Nakagami fading channels. The main contributions are listed as follows:

1. Closed-form expressions are provided for the PDF and cumulative density functions (CDF) of the SNR over N-Nakagami fading channels. These are used to derive exact ASEP expressions.

2. The exact closed-form OP expressions for an SDC system are also derived.

3. The ASEP and OP performance under different conditions is evaluated through numerical simulation to verify the analysis. Results are presented which show that the performance of the SDC system is improved when the number of diversity branches and the fading coefficient is increased, but is degraded as the number of cascaded components is increased.

4. The derived ASEP and OP expressions can be used to evaluate the ASEP and OP performance of the vehicular communications, such as inter-vehicular communications, intelligent highway applications and mobile ad-hoc applications.

The rest of the paper is organized as follows. The SDC system model is presented in Section 2. Section 3 provides exact and approximate ASEP expressions for phase shift keying (PSK) and pulse amplitude modulation (PAM). Exact closed-form OP expressions are presented in Section 4. Monte Carlo simulation is used in Section 5 to confirm the analytical results in the previous sections. Finally, some concluding remarks are given in Section 6.

2. System Model

Z follows N-Nakagami distribution, which can be represented by a product of N independent random variables [4]

$$Z = \prod_{i=1}^{N} a_i \tag{1}$$

where N is the number of cascaded components, and a_i is a Nakagami distributed random variable with PDF as

$$f(a) = \frac{2m^m}{\Omega^m \Gamma(m)} a^{2m-1} \exp\left(-\frac{m}{\Omega} a^2\right) \tag{2}$$

$\Gamma(\cdot)$ is the Gamma function, m is the fading coefficient and Ω is a scaling factor. According to [4], the PDF of Z is given as

$$f(z) = \frac{2}{z\prod_{i=1}^{N} \Gamma(m_i)} G_{0,N}^{N,0}\left[z^2 \prod_{i=1}^{N} \frac{m_i}{\Omega_i} \middle|_{m_1,\ldots,m_N}^{-} \right] \tag{3}$$

where $G[\cdot]$ is Meijer's G-function.

Now consider an SDC system over an N-Nakagami fading channel with additive white Gaussian noise (AWGN). We assume there are L independent diversity branches. The instantaneous SNR of the jth branch is given by [14]

$$r_j = \left|Z_j\right|^2 \frac{E_s}{N_0}, \; j = 1, \ldots, L \tag{4}$$

where E_s is the average transmitted symbol energy and N_0 is the single-sided AWGN power spectral density.

The corresponding average SNR is given as [14]

$$\overline{r_j} = E\left(\left|Z_j\right|^2\right) \frac{E_s}{N_0}, \; j = 1, \ldots, L \tag{5}$$

where $E(\cdot)$ denotes expectation.

The CDF of r_j can be expressed as [4]

$$F_{r_j}(r) = \frac{1}{\prod_{i=1}^{N} \Gamma(m_i)} G_{1,N+1}^{N,1}\left[\frac{r}{r_j} \prod_{i=1}^{N} m_i \middle|_{m_1,\ldots,m_N,0}^{1} \right] \tag{6}$$

Taking the first derivative of (6) with respect to r gives the corresponding PDF as [4]

$$f_{r_j}(r) = \frac{1}{r\prod_{i=1}^{N} \Gamma(m_i)} G_{0,N}^{N,0}\left[\frac{r}{r_j} \prod_{i=1}^{N} m_i \middle|_{m_1,\ldots,m_N}^{-} \right] \tag{7}$$

First consider the case where the branches are independent and identically distributed, with PDF and CDF given by (6) and (7), respectively. The average SNR can then be written as

$$\overline{r} = \overline{r_j} \tag{8}$$

The PDF of r_{SSC} is given as [10]

$$f_{SSC}(r) = \begin{cases} F_r(r_{th})\, f_r(r) & 0 < r < r_{th} \\ [1 + F_r(r_{th})]\, f_r(r) & r \geq r_{th} \end{cases} \tag{9}$$

where $f_r(\cdot)$ and $F_r(\cdot)$ are the PDF and CDF of the instantaneous SNR for a diversity branch, and r_{th} is the switching threshold.

The PDF of r_{SEC} is given as [10]

$$f_{SEC}(r)=\begin{cases}\left[F_r(r_{th})\right]^{L-1} f_r(r) & 0<r<r_{th}\\ \dfrac{\left[F_r(r_{th})\right]^{L}-1}{F_r(r_{th})-1} f_r(r) & r\geq r_{th}\end{cases} \tag{10}$$

This shows that the PDF of r_{SEC} does not depend on the number of diversity branches L. The PDF of r_{SEC} has the same expressions as the PDF of r_{SSC} when $L = 2$. Thus we only need to analyze an SEC in the remainder of this paper.

3. The ASEP Performance

The SEP averaged over the fading SNR is given by [15]

$$P=\int_0^{\infty} P_q(r)\, f_{SEC}(r)\, dr \tag{11}$$

where $P_q(x)$ denotes the SEP of the q-ary modulation employed. We first consider q-ary PAM and then q-ary PSK.

A. PAM

The SEP of q-ary PAM modulation in an additive white Gaussian noise (AWGN) channel is given by [15]

$$P_q(r)=2\left(1-\frac{1}{q}\right)Q\left(\sqrt{\frac{6r}{q^2-1}}\right) \tag{12}$$

Substituting (10) and (12) into (11), the ASEP of q-ary PAM over N-Nakagami fading channels is

$$\begin{aligned}P_{PAM}&=2\left(1-\frac{1}{q}\right)\left\{\begin{array}{l}\left[F_r(r_{th})\right]^{L-1}\int_0^{r_{th}} Q\left(\sqrt{\frac{6r}{q^2-1}}\right) f_r(r)\,dr\\ +\dfrac{\left[F_r(r_{th})\right]^{L}-1}{F_r(r_{th})-1}\int_{r_{th}}^{\infty} Q\left(\sqrt{\frac{6r}{q^2-1}}\right) f_r(r)\,dr\end{array}\right\}\\ &=2\left(1-\frac{1}{q}\right)\left\{\begin{array}{l}\left[F_r(r_{th})\right]^{L-1}\int_0^{\infty} Q\left(\sqrt{\frac{6r}{q^2-1}}\right) f_r(r)\,dr\\ +\dfrac{\left[F_r(r_{th})\right]^{L-1}-1}{F_r(r_{th})-1}\int_{r_{th}}^{\infty} Q\left(\sqrt{\frac{6r}{q^2-1}}\right) f_r(r)\,dr\end{array}\right\}\\ &=2\left(1-\frac{1}{q}\right)\left(\left[F_r(r_{th})\right]^{L-1} G_1+\frac{\left[F_r(r_{th})\right]^{L-1}-1}{F_r(r_{th})-1} G_2\right)\end{aligned} \tag{13}$$

By the help of [16, eq. 21], G_1 can be given as

$$G_1 = \frac{1}{\prod_{i=1}^{N}\Gamma(m_i)}\int_0^{\infty} Q\left(\sqrt{\frac{6r}{q^2-1}}\right)\frac{1}{r}G_{0,N}^{N,0}\left[\frac{r}{r}=\prod_{i=1}^{N} m_i \middle| \begin{matrix} - \\ m_1,\ldots,m_N \end{matrix}\right]dr$$

$$= \frac{1}{2\prod_{i=1}^{N}\Gamma(m_i)}\int_0^{\infty} \operatorname{erfc}\left(\sqrt{\frac{3r}{q^2-1}}\right)\frac{1}{r}G_{0,N}^{N,0}\left[\frac{r}{r}=\prod_{i=1}^{N} m_i \middle| \begin{matrix} - \\ m_1,\ldots,m_N \end{matrix}\right]dr$$

$$= \frac{1}{2\sqrt{\pi}\prod_{i=1}^{N}\Gamma(m_i)}\int_0^{\infty} r^{-1}G_{1,2}^{2,0}\left[\frac{3r}{q^2-1}\middle| \begin{matrix} 1 \\ 0,\frac{1}{2} \end{matrix}\right]G_{0,N}^{N,0}\left[\frac{r}{r}=\prod_{i=1}^{N} m_i \middle| \begin{matrix} - \\ m_1,\ldots,m_N \end{matrix}\right]dr \quad (14)$$

$$= \frac{1}{2\sqrt{\pi}\prod_{i=1}^{N}\Gamma(m_i)}G_{2,N+1}^{N,2}\left[\frac{q^2-1}{3r}\prod_{i=1}^{N} m_i \middle| \begin{matrix} 1,\frac{1}{2} \\ m_1,\cdots,m_N,0 \end{matrix}\right]$$

Next, G_2 is evaluated.

$$G_2 = \int_{r_{th}}^{\infty} Q\left(\sqrt{\frac{6r}{q^2-1}}\right) f_r(r)dr$$

$$= \frac{1}{2}\int_{r_{th}}^{\infty} erfc\left(\sqrt{\frac{3r}{q^2-1}}\right) f_r(r)dr$$

$$= \frac{1}{2}\left\{ erfc\left(\sqrt{\frac{3r}{q^2-1}}\right)F_r(r)\Big|_{r_{th}}^{\infty} - \int_{r_{th}}^{\infty} erfc'\left(\sqrt{\frac{3r}{q^2-1}}\right)F_r(r)dr \right\}$$

$$= \frac{1}{2}\left\{ erfc\left(\sqrt{\frac{3r}{q^2-1}}\right)F_r(r)\Big|_{r_{th}}^{\infty} + \frac{3}{q^2-1}\int_{r_{th}}^{\infty} \frac{\exp\left(-\frac{3r}{q^2-1}\right)}{\sqrt{\frac{3\pi r}{q^2-1}}}F_r(r)dr \right\} \quad (15)$$

and substituting (6) into (15) gives

$$G_2 = \frac{1}{2}\left\{-erfc\left(\sqrt{\frac{3r_{th}}{q^2-1}}\right)F_r(r_{th}) + \sqrt{\frac{3}{(q^2-1)\pi}}\int_{r_{th}}^{\infty}\frac{\exp\left(-\frac{3r}{q^2-1}\right)}{\sqrt{r}}F_r(r)dr\right\}$$

$$= \frac{1}{2}\left\{\begin{array}{l}\frac{\sqrt{\frac{3}{(q^2-1)\pi}}}{\prod_{i=1}^{N}\Gamma(m_i)}\int_0^{\infty}\frac{\exp\left(-\frac{3r}{q^2-1}\right)}{\sqrt{r}}G_{1,N+1}^{N,1}\left[\frac{r}{r}\prod_{i=1}^{N}m_i\middle|_{m_1,\ldots,m_N,0}^{1}\right]dr \\ -erfc\left(\sqrt{\frac{3r_{th}}{q^2-1}}\right)F_r(r_{th}) - \frac{\sqrt{\frac{3}{(q^2-1)\pi}}}{\prod_{i=1}^{N}\Gamma(m_i)}\times \\ \int_0^{r_{th}}\frac{\exp\left(-\frac{3r}{q^2-1}\right)}{\sqrt{r}}G_{1,N+1}^{N,1}\left[\frac{r}{r}\prod_{i=1}^{N}m_i\middle|_{m_1,\ldots,m_N,0}^{1}\right]dr\end{array}\right\} \quad (16)$$

$$= \frac{1}{2}\left\{\begin{array}{l}\frac{1}{\sqrt{\pi}\prod_{i=1}^{N}\Gamma(m_i)}G_{2,N+1}^{N,2}\left[\frac{q^2-1}{3r}\prod_{i=1}^{N}m_i\middle|_{m_1,\ldots,m_N,0}^{\frac{1}{2},1}\right] - \\ erfc\left(\sqrt{\frac{3r_{th}}{q^2-1}}\right)G_{1,N+1}^{N,1}\left[\frac{r_{th}}{r}\prod_{i=1}^{N}m_i\middle|_{m_1,\ldots,m_N,0}^{1}\right] - \frac{\sqrt{\frac{3}{(q^2-1)\pi}}}{\prod_{i=1}^{N}\Gamma(m_i)}GG_1\end{array}\right\}$$

Next, GG_1 is evaluated. We can rewrite the Meijer's G-function as [17, eq.9.303]

$$\begin{aligned}&G_{1,N+1}^{N,1}\left[\frac{r}{r}\prod_{i=1}^{N}m_i\middle|_{m_1,\cdots,m_N,0}^{1}\right] \quad (17)\\ &= \sum_{h=1}^{N}\frac{\prod_{j=1}^{N}\Gamma(m_j-m_h)\Gamma(m_h)}{\Gamma(1+m_h)}\left(\frac{r}{r}\prod_{i=1}^{N}m_i\right)^{m_h}{}_1F_N(m_h;1+m_h-m_1,\ldots,1+m_h;(-1)^N\frac{r}{r}\prod_{i=1}^{N}m_i)\\ &= \sum_{h=1}^{N}\frac{\prod_{j=1}^{N}\Gamma(m_j-m_h)\Gamma(m_h)}{\Gamma(1+m_h)}\times\sum_{k=0}^{\infty}\frac{(-1)^{Nk}\left(\frac{1}{r}\prod_{i=1}^{N}m_i\right)^{k+m_h}(m_h)_k}{(1+m_h-m_1)_k(1+m_h-m_2)_k\ldots(1+m_h)_k}\frac{r^{k+m_h}}{k!}\end{aligned}$$

where

$$\begin{aligned}&{}_pF_q(\alpha_1,\alpha_2,\ldots,\alpha_p;\beta_1,\beta_2,\ldots,\beta_q;z)\\ &= \sum_{k=0}^{\infty}\frac{(\alpha_1)_k(\alpha_2)_k\ldots(\alpha_p)_k}{(\beta_1)_k(\beta_2)_k\ldots(\beta_q)_k}\frac{z^k}{k!}\end{aligned} \quad (18)$$

$$(x)_k = \prod_{t=0}^{k-1}(x+t),(x)_0 = 1 \quad (19)$$

Substituting (17) into (16), we can obtain

$$\begin{aligned}GG_1 = &\sum_{h=1}^{N}\frac{\prod_{j=1}^{N}\Gamma(m_j-m_h)\Gamma(m_h)}{\Gamma(1+m_h)}\times\\ &\sum_{k=0}^{\infty}\frac{(-1)^{Nk}\left(\frac{1}{r}\prod_{i=1}^{N}m_i\right)^{k+m_h}(m_h)_k}{(1+m_h-m_1)_k(1+m_h-m_2)_k\ldots(1+m_h)_k}\frac{1}{k!}\\ &\times\left(\frac{3}{q^2-1}\right)^{-(k+m_h+0.5)}\gamma\left(k+m_h+0.5,\frac{3r_{th}}{q^2-1}\right)\end{aligned} \quad (20)$$

where

$$\gamma(\alpha, x) = \int_0^x \exp(-t)t^{\alpha-1}dt, \mathrm{Re}(\alpha) > 0 \tag{21}$$

B. PSK

The SEP of *q*-ary PSK modulation in an AWGN channel is given by [14]

$$P_q(r) = 2Q\left(\sqrt{2\sin^2\frac{\pi}{q}r}\right) - \frac{1}{\pi}\int_{\frac{\pi}{2}-\frac{\pi}{q}}^{\frac{\pi}{2}} e^{-r\frac{\sin^2\pi/q}{\cos^2\theta}}d\theta \tag{22}$$

For large SNRs and large values of *q*, the SEP of *q*-ary PSK can be approximated as

$$P_q(r) \approx 2Q\left(\sqrt{2\sin^2\frac{\pi}{q}r}\right) \tag{23}$$

Substituting (23) into (11), the ASEP of *q*-ary PSK over *N*-Nakagami fading channels can be approximated as

$$\begin{aligned} P_{PSK}(r) &\approx \int_0^\infty 2Q\left(\sqrt{2\sin^2\frac{\pi}{q}r}\right) f_{SEC}(r)dr \\ &= 2\left\{\begin{array}{l}\left[F_r(r_{th})\right]^{L-1}G_{11} \\ +\dfrac{\left[F_r(r_{th})\right]^{L-1}-1}{F_r(r_{th})-1}G_{22}\end{array}\right\} \end{aligned} \tag{24}$$

where

$$\begin{aligned} G_{11} &= \int_0^\infty Q\left(\sqrt{2\sin^2\frac{\pi}{q}r}\right) f_r(r)dr \\ &= \frac{1}{2\sqrt{\pi}\prod_{i=1}^{N}\Gamma(m_i)}G_{2,N+1}^{N,2}\left[\frac{1}{\sin^2\frac{\pi}{q}r}\prod_{i=1}^{N}m_i \middle| \begin{matrix}1,\frac{1}{2} \\ m_1,\cdots,m_N,0\end{matrix}\right] \end{aligned} \tag{25}$$

and

$$G_{22} = \frac{1}{2}\left\{\begin{array}{l}\dfrac{1}{\sqrt{\pi}\prod_{i=1}^{N}\Gamma(m_i)}G_{2,N+1}^{N,2}\left[\dfrac{1}{\sin^2\frac{\pi}{q}r}\prod_{i=1}^{N}m_i \middle| \begin{matrix}\frac{1}{2},1 \\ m_1,\ldots,m_N,0\end{matrix}\right] - \\ erfc\left(\sqrt{\sin^2\frac{\pi}{q}r_{th}}\right)G_{1,N+1}^{N,1}\left[\dfrac{r_{th}}{r}\prod_{i=1}^{N}m_i \middle| \begin{matrix}1 \\ m_1,\ldots,m_N,0\end{matrix}\right] - \dfrac{\sqrt{\frac{\sin^2\frac{\pi}{q}}{\pi}}}{\prod_{i=1}^{N}\Gamma(m_i)}GG_2\end{array}\right\} \tag{26}$$

where

$$GG_2 = \sum_{h=1}^{N} \frac{\prod_{j=1}^{N} \Gamma(m_j - m_h)\Gamma(m_h)}{\Gamma(1+m_h)} \times$$
$$\sum_{k=0}^{\infty} \frac{(-1)^{Nk} (\frac{1}{r} \prod_{i=1}^{N} m_i)^{k+m_h} (m_h)_k}{(1+m_h-m_1)_k (1+m_h-m_2)_k \ldots (1+m_h)_k} \frac{1}{k!} \quad (27)$$
$$\times (\sin^2 \frac{\pi}{q})^{-(k+m_h+0.5)} \gamma(k+m_h+0.5, \sin^2 \frac{\pi}{q} r_{th})$$

4. The OP Performance

The OP is given by [14]

$$P_{out} = \Pr[0 \le r \le r_T] = \int_0^{r_T} f_{SEC}(r) dr \quad (28)$$

where r_T is a given threshold for correct detection.

Substituting (10) into (28) results in

$$P_{out} = \begin{cases} [F_r(r_{th})]^{L-1} F_r(r_T) & 0 < r_T < r_{th} \\ \frac{F_r(r_{th}) - [F_r(r_{th})]^L}{F_r(r_{th}) - 1} + \frac{[F_r(r_{th})]^L - 1}{F_r(r_{th}) - 1} F_r(r_T) & r_T \ge r_{th} \end{cases} \quad (29)$$

5. Numerical Results

In this section, we present Monte-Carlo simulations and numerical methods to confirm the derived analytical results. The simulation results are obtained for BPAM and QPSK modulations. Additionally, random number simulation was done to confirm the validity of the analytical approach. All the computations were done in MATLAB and some of the integrals were verified through MAPLE. The number of diversity branches is L=1,2,3,4, the fading coefficient is m=1,2,3, and the number of cascaded components is N=2,3,4.

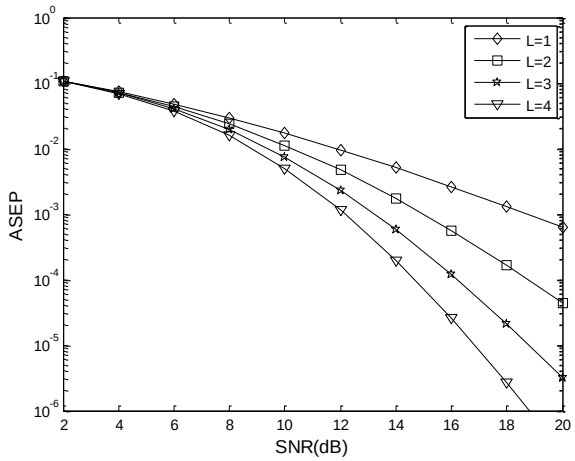

Figure 1. The Effect of the Diversity Branches *L* on the ASEP Performance

Figure 1 presents the ASEP performance of an SDC system over *N*-Nakagami fading channels with BPAM modulation. The number of cascaded components is *N*=2, and the number of diversity branches is *L*=1, 2, 3, 4. When *L*=2, SEC is equivalent to SSC. The fading coefficient is *m*=2 and the switching threshold r_{th} is 10dB. These results show that the ASEP performance is improved as the number of diversity branches *L* is increased. For example, when SNR=16dB, for *L*=1 the ASEP is 2.6×10^{-3}, for *L*=2 the ASEP is 5.6×10^{-4}, for *L*=3 the ASEP is 1.2×10^{-4}, and for *L*=4 the ASEP is 2.6×10^{-5}. For fixed *L*, an increase in the SNR reduces the ASEP over *N*-Nakagami fading channels.

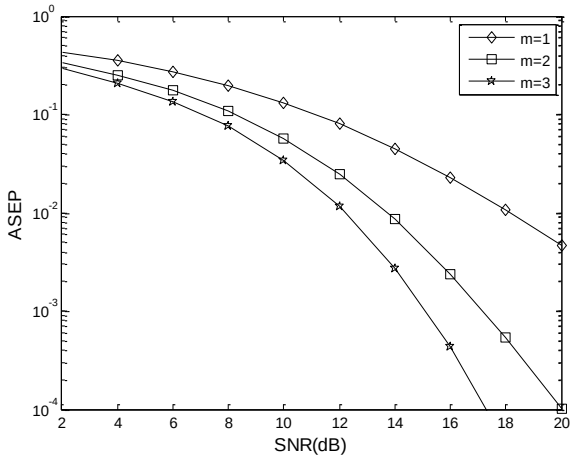

Figure 2. The Effect of the Fading Coefficient *m* on the ASEP Performance

Figure 2 presents the ASEP performance of an SDC system over *N*-Nakagami fading channels with QPSK modulation. The number of cascaded components is *N*=2, the number of diversity branches is *L*=3, and the fading coefficient is *m*=1, 2, 3. The switching threshold r_{th} is 13dB. These results show that the ASEP is improves as the fading coefficient *m* increases. For example, when SNR=12 dB, for *m* =1 the ASEP is 8.1×10^{-2}, for *m* =2 the ASEP is 2.5×10^{-2}, and for *m* =3 the ASEP is 1.2×10^{-2}. This is because the fading severity of an *N*-Nakagami channel is reduced with a larger *m*. For fixed *m*, an increase in the SNR reduces the ASEP over *N*-Nakagami fading channels, as expected.

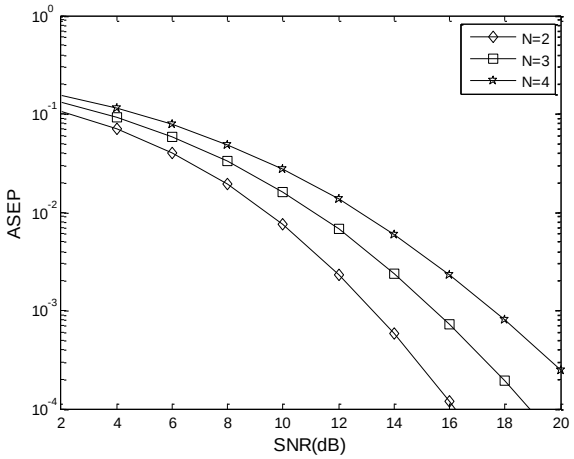

Figure 3. The Effect of the Number of Cascaded Components *N* on the ASEP Performance

Figure 3 presents the ASEP performance of an SDC system over *N*-Nakagami fading channels with BPAM modulation. The number of cascaded components is *N*=2, 3, 4,

which corresponds to double-Nakagami, 3-Nakagami, and 4-Nakagami fading channels, respectively. The number of diversity branches is L=3, and the fading coefficient is m=2. The switching threshold r_{th} is 10dB. These results show that the ASEP is degraded as N increases. For example, when SNR=12dB, for N=2, the ASEP is 2.3×10^{-3}, for N=3 the ASEP is 6.7×10^{-3}, and for N=4 the ASEP is 1.4×10^{-2}.This is because the fading severity of the cascaded channels increases as N increases. For fixed N, an increase in the SNR reduces the ASEP, as expected.

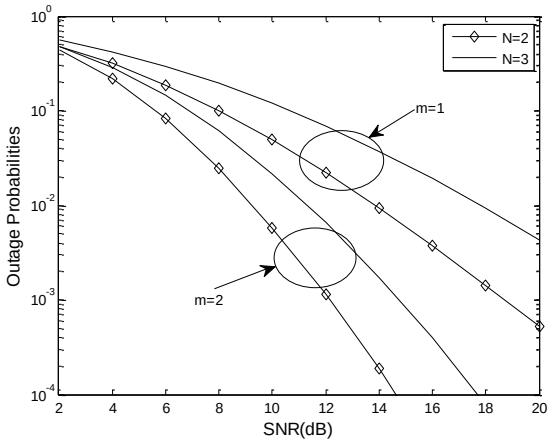

Figure 4. The OP for an SDC System over *N*-Nakagami Fading Channels

Figure 4 presents the OP performance of an SDC system over N-Nakagami fading channels. The number of cascaded components is N=2, 3, the number of diversity branches is L=3, and the fading coefficient is m=1, 2, respectively. The switching threshold r_{th} is 4dB, and r_T is 2dB. These results show that the OP improves as the fading coefficient m is increased. For example, when SNR=12 dB and N=2, for m=1 the OP is 2×10^{-2}, and for m=2 the OP is 1×10^{-3}. Further, an increase in the number of cascaded components N degrades the OP performance. For example, when SNR=12 dB and m=2, for N =2 the OP is 1×10^{-3}, and for N =3 the OP is 6×10^{-3}. For fixed N and m, an increase in the SNR results in a reduced OP over N-Nakagami fading channels.

6. Conclusion

The ASEP and OP performance of an SDC system over N-Nakagami fading channels is investigated in this paper. Exact and approximate ASEP and OP expressions are derived. Performance results are presented which show that the number of diversity branches L, the fading coefficient m, and the number of cascaded components N have an important impact on the ASEP and OP performance. The derived ASEP and OP expressions can be used to evaluate the ASEP and OP performance of the vehicular communication systems such as inter-vehicular communications, intelligent highway applications and mobile ad-hoc applications. In the future, we will consider the impact of the correlated channels on the ASEP and OP performance.

Acknowledgments

The authors would like to thank the referees and editors for providing very helpful comments and suggestions. This project was supported by National Natural Science Foundation of China (no. 61304222, no. 61301139), Natural Science Foundation of Shandong Province (no. ZR2012FQ021), Shandong Province Outstanding Young Scientist Award Fund (no. 2014BSE28032).

References

[1] A. T. Gamage, H. Liang, R. Zhang and X. Shen, "Device-to-device communication underlaying converged heterogeneous networks", IEEE Wireless Communications, vol. 21, no. 6, **(2014)**, pp. 98-107.
[2] K. W. Yang, M. Wang, K. J. Zou, M. Hua, J. J. Hu, J. Zhang, W. Sheng and X. You, "Device discovery for multihop cellular networks with its application in LTE", IEEE Wireless Communications, vol. 21, no.5, **(2014)**, pp. 24-34.
[3] M. Uysal, "Diversity analysis of space-time coding in cascaded Rayleigh fading channels", IEEE Communications Letters, vol. 10, no. 3, **(2006)**, pp. 165-167.
[4] G. K. Karagiannidis, N. C. Sagias and P. T. Mathiopoulos, "N*Nakagami: a novel stochastic model for cascaded fading channels", IEEE Transactions on Communications, vol. 55, no. 8, **(2007)**, pp. 1453-1458.
[5] F. K. Gong, P. Ye, Y. Wang and N. Zhang, "Cooperative mobile-to-mobile communications over double Nakagami-m fading channels", IET Communications, vol. 6, no. 18, **(2012)**, pp. 3165-3175.
[6] S. Mumtaz, K.M. S. Huq, J. Rodriguez. "Direct mobile-to-mobile communication: Paradigm for 5G," IEEE Wireless Communications, vol. 21, no.5, pp. 14-23, (**2014**).
[7] Z. Fang, X. Yuan, and X. Wang, "Towards the asymptotic sum capacity of the MIMO cellular two-way relay channel, " IEEE Transactions on Signal Processing, vol. 62, no. 6,pp. 4039-4051, (**2014**).
[8] D. Molteni, M. Nicoli, and U. Spagnolini, "Performance of MIMO-OFDMA systems in correlated fading channels and non-stationary interference, " IEEE Transactions on Wireless Communications, vol. 10, no. 5, pp. 1480-1494, (**2011**).
[9] X. Yuan, T. Yang, and I. B. Collings. "Multiple-input multiple-output two-way relaying: a space-division approach, "IEEE Transactions on Information Theory, vol. 59, no. 5, pp. 6421-6440, (**2013**).
[10] L. Xiao and X. Dong, "New results on the BER of switched diversity combining over Nakagami fading channels, " IEEE Communications Letters, vol. 9, no. 2,pp. 136-138, (**2005**).
[11] B.R.Manoj, and P.R.Sahu. "Performance analysis of dual-'switch and stay' combiner over correlated K_G fading channels, " Proceedings of the International Conference on Communications, New Delhi, India, **(2013)**,pp. 1-5.
[12] D. M.Jiménez, J. F. Paris, and K.K. Wong, "Closed-form analysis of multi-branch switched diversity with noncoherent and differentially coherent detection," International Journal of Communication Systems, vol. 26, no.1, pp. 127-137, **(2013)**.
[13] S. Khatalin. "Performance analysis of switch and stay combining diversity system over κ-μ fading channels, "International Journal of Electronics and Communications, vol. 69, no. 2, pp. 475-486, **(2015)**.
[14] M. K. Simon, and M.S. Alouini. "Digital Communication over Fading Channels", 2th ed., Wiley, New York, **(2004)**.
[15] J. G. Proakis. "Digital Communications" , 4th ed., McGraw-Hill, New York, **(2001)**.
[16] V. S. Adamchik, and O. I. Marichev. "The algorithm for calculating integrals of hypergeometric type functions and its realization in reduce system, " Proceedings of the International Symposium on Symbolic and Algebraic Computation, Tokyo, Japan, **(1990)**,pp. 212-224.
[17] I. S. Gradshteyn, and I. M. Ryzhik. "Table of Integrals, Series, and Products", 5th ed., Academic Press, San Diego, CA, **(1994)**.

Authors

Lingwei Xu was born in Gaomi, Shandong Province, China, in 1987. He received his B.E. degree in Communication Engineering from Qingdao Technological University, China in 2011. He received his M.E. degree in Electronics and Communication Engineering from Ocean University of China, China in 2013. Now he is a Ph.D. candidate in Ocean University of China. His research interests include ultra-wideband radio systems, MIMO wireless systems, and M2M wireless communications.

Jingjing Wang was born in Anhui, China, in 1975. She received her B.S. degree in Industrial Automation from Shandong University, Jinan, China, in 1997, the M.S. degree in Control Theory and Control Engineering, Qingdao University of Science & Technology, Qingdao, China, in 2002, and the Ph.D. degree in Computer Application Technology, Ocean University of China, Qingdao, China, in 2012. From 2002 to now, she is an associate professor at

the College of Information Science & Technology, Qingdao University of Science & Technology. Her research interests include 60GHz wireless communication, 60GHz wireless position technology, ultra-wideband radio systems, and cooperative communication networks.

Hao Zhang received his B.E. degree in Telecommunications Engineering and Industrial Management from Shanghai Jiaotong University, China in 1994. He received his MBA degree from New York Institute of Technology, USA in 2001. He received his Ph.D. degree in Electrical and Computer Engineering from the University of Victoria, Canada in 2004. From 1994 to 1997, he was the Assistant President of ICO Global Communication Company. In 2000, he joined Microsoft Canada as a Software Engineer, and was Chief Engineer at Dream Access Information Technology, Canada from 2001 to 2002. He is currently a professor in the Department of Electronic Engineering at Ocean University of China and an adjunct professor in the Department of Electrical and Computer Engineering at the University of Victoria. His research interests include ultra-wideband radio systems, MIMO wireless systems, cooperative communication networks and spectrum communications.

T. Aaron Gulliver received his Ph.D. degree in Electrical and Computer Engineering from the University of Victoria, Victoria, BC, Canada in 1989. He is a professor in the Department of Electrical and Computer Engineering. From 1989 to 1991 he was employed as a Defense Scientist at Defense Research Establishment Ottawa, Ottawa, ON, Canada. He has held academic positions at Carleton University, Ottawa, and the University of Canterbury, Christchurch, New Zealand. He joined the University of Victoria in 1999 and is a Professor in the Department of Electrical and Computer Engineering. In 2002 he became a Fellow of the Engineering Institute of Canada, and in 2012 a Fellow of the Canadian Academy of Engineering. He is also a senior member of IEEE. His research interests include information theory and communication theory, and ultra wideband communication.

